

**\*\*\* PROOF OF YOUR ARTICLE ATTACHED, PLEASE READ CAREFULLY \*\*\***

After receipt of your corrections your article will be published initially within the online version of the journal.

**PLEASE NOTE THAT THE PROMPT RETURN OF YOUR PROOF CORRECTIONS WILL ENSURE THAT THERE ARE NO UNNECESSARY DELAYS IN THE PUBLICATION OF YOUR ARTICLE**

**READ PROOFS CAREFULLY**

**ONCE PUBLISHED ONLINE OR IN PRINT IT IS NOT POSSIBLE TO MAKE ANY FURTHER CORRECTIONS TO YOUR ARTICLE**

- § This will be your only chance to correct your proof
- § Please note that the volume and page numbers shown on the proofs are for position only

**ANSWER ALL QUERIES ON PROOFS** (Queries are attached as the last page of your proof.)

- § List all corrections and send back via e-mail to the production contact as detailed in the covering e-mail, or mark all corrections directly on the proofs and send the scanned copy via e-mail. Please do not send corrections by fax or post

**CHECK FIGURES AND TABLES CAREFULLY**

- § Check sizes, numbering, and orientation of figures
- § All images in the PDF are downsampled (reduced to lower resolution and file size) to facilitate Internet delivery. These images will appear at higher resolution and sharpness in the printed article
- § Review figure legends to ensure that they are complete
- § Check all tables. Review layout, titles, and footnotes

**COMPLETE COPYRIGHT TRANSFER AGREEMENT (CTA) if you have not already signed one**

- § Please send a scanned signed copy with your proofs by e-mail. **Your article cannot be published unless we have received the signed CTA**

**OFFPRINTS**

- § 25 complimentary offprints of your article will be dispatched on publication. Please ensure that the correspondence address on your proofs is correct for dispatch of the offprints. If your delivery address has changed, please inform the production contact for the journal – details in the covering e-mail. Please allow six weeks for delivery.

**Additional reprint and journal issue purchases**

- § Should you wish to purchase a minimum of 100 copies of your article, please visit [http://www3.interscience.wiley.com/aboutus/contact\\_reprint\\_sales.html](http://www3.interscience.wiley.com/aboutus/contact_reprint_sales.html)
- § To acquire the PDF file of your article or to purchase reprints in smaller quantities, please visit <http://www3.interscience.wiley.com/aboutus/ppv-articleselect.html>. Restrictions apply to the use of reprints and PDF files – if you have a specific query, please contact [permreq@wiley.co.uk](mailto:permreq@wiley.co.uk). Corresponding authors are invited to inform their co-authors of the reprint options available
- § To purchase a copy of the issue in which your article appears, please contact [cs-journals@wiley.co.uk](mailto:cs-journals@wiley.co.uk) upon publication, quoting the article and volume/issue details
- § Please note that regardless of the form in which they are acquired, reprints should not be resold, nor further disseminated in electronic or print form, nor deployed in part or in whole in any marketing, promotional or educational contexts without authorization from Wiley. Permissions requests should be directed to <mailto:permreq@wiley.co.uk>

## Smoothing and bootstrapping the PROMETHEUS fire growth model

Tanya Garcia<sup>1</sup>, John Braun<sup>2\*,†</sup>, Robert Bryce<sup>3</sup> and Cordy Tymstra<sup>4</sup>

<sup>1</sup>*Université de Neuchâtel, Institute of Statistics, Pierre à Mazel, 7, 2002 Neuchâtel, Switzerland*

<sup>2</sup>*Department of Statistical and Actuarial Sciences, The University of Western Ontario, London, Ontario, Canada N6A 5B7*

<sup>3</sup>*Box 333, Austin, Manitoba, Canada R0H 0C0*

<sup>4</sup>*Wildfire Science Supervisor, Forestry Business Services Branch, Forestry Division, Department of Sustainable Resource Development, 9th Floor, 9920 – 108 Street, Edmonton, Alberta, Canada T5K 2M4*

### SUMMARY

The PROMETHEUS model is a spatially explicit, deterministic fire growth model, praised for being beneficial in various aspects of fire management. Our goal is to build on this success, applying statistical smoothing to alleviate some computational difficulties and to increase accuracy; a pleasant by-product is the opportunity to introduce stochasticity to the model using a residual-based block bootstrap. Copyright © 2007 John Wiley & Sons, Ltd.

KEY WORDS: PROMETHEUS; smoothing; bootstrapping; fire growth; stochasticity

### 1. INTRODUCTION

Having a high density of forests, Canada is highly susceptible to fire disasters. In fact, the last three decades have shown an upward trend in area burned by wildland fires, and since 1980, the mean annual area burned in Canada is 2.5 million hectares (Podur *et al.*, 2002; Gillett *et al.*, 2004). To help prevent further loss, in April 1999, the foothills model forest (FMF) received a proposal for the design of a wildland fire growth model. In response, the Alberta Forest Protection Branch designed PROMETHEUS—a spatially explicit, deterministic fire growth model, now considered Canada's leading fire management tool (Forestry Canada Fire Danger Group, 1992).

To model fire growth accurately, PROMETHEUS considers the factors that most affect a fire's rate of spread and its shape:

- (1) Fuel type and moisture content;
- (2) Wind speed;
- (3) Topography, fires spread faster uphill and cannot traverse natural barriers;

\*Correspondence to: J. Braun, Department of Statistical and Actuarial Sciences, The University of Western Ontario, London, Ontario, Canada N6A 5B7.

†E-mail: braun@stats.uwo.ca

- (4) Fuel continuity, i.e. whether the fuel is sparse or homogeneous, also whether the fuel is of constant or variable type; and
- (5) The amount of spotting, i.e. burning material spread by the wind.

Data have been collected from experimental burns and well-documented wildfires with continuous uniform fuels involving constant wind velocity, moisture content and slope. Under these conditions, a fire from its ignition point will reach a quasi-steady state, and progress at a constant rate as a cigar shape biased toward the downward direction. In general, one approximates the fire growth with an elliptical shape. Other variations include teardrops, ovoids and double ellipses, where these shapes result from varying topography and sparse fuels. For our analysis, we assume an elliptical shape.

The factors used to model fire growth in PROMETHEUS are obtained from the the Canadian Forest Fire Behaviour Prediction System (Forestry Canada Fire Danger Group, 1992). The FBP System measures the rate of spread, fuel consumption, head fire intensity, fire type and crown fraction burned based on fuels, weather, topography, foliar moisture content and the type and duration of the predicted fire front.

Although PROMETHEUS is well established and utilized frequently by Canada's wildfire management, challenges remain to manage vertex behaviours during propagation. Among these are the knots and crossovers that occur in representing fire perimeters; these complications may produce unrealistic fire fronts and incur computation errors. This paper discusses the use of smoothed data to reduce some of the complications present in the PROMETHEUS output. Essentially, smoothing the data used to calculate the parameter values will reduce measurement error (some of which may be induced by the grid itself), and to remove the magnitude of discontinuities present in the data. Smoothing is also believed to reduce the knots that occur; this in addition to an 'untangling' heuristic can improve the PROMETHEUS model. Lastly, using a block bootstrap procedure, we demonstrate a way to introduce stochasticity to the deterministic PROMETHEUS model.

The contents of this paper are as follows: factors to consider for modelling fire growth; description of the differential spread equations for PROMETHEUS; the algorithm proposed and implemented as PROMETHEUS; an explanation of how smoothing can be applied to the input parameters in PROMETHEUS and implementing the block bootstrap to obtain a stochastic spread model.

## 2. DIFFERENTIAL SPREAD EQUATIONS USING HUYGENS' PRINCIPLE

In 1990, Gwynfor Richards at Brandon University proposed a model for forest fire propagation. Today, it is well accepted from both the theoretical and applied points of view (see Bryce and Richards, 1995; Richards, 1988, 1990, 1995). Richards' model is set in a two-dimensional spatial domain and takes into account the outputs from the FBP System. The three-dimensional effects of slope and topography are incorporated into the two-dimensional model via a projection method. Hence, the fire spreads as if it were evolving on a topographical map of the terrain, with the slope accounted for by the non-homogeneity of the spatial domain and model parameters.

Assuming a locally smooth fire front and using Huygens' principle, the model states that each point on the fire front is an ignition point for a small fire that burns out an elliptical region in a finite time interval. The envelope of these ellipses defines the new fire front at the next time instant. This evolution is modelled by Richards' set of differential equations (see Richards, 1990).

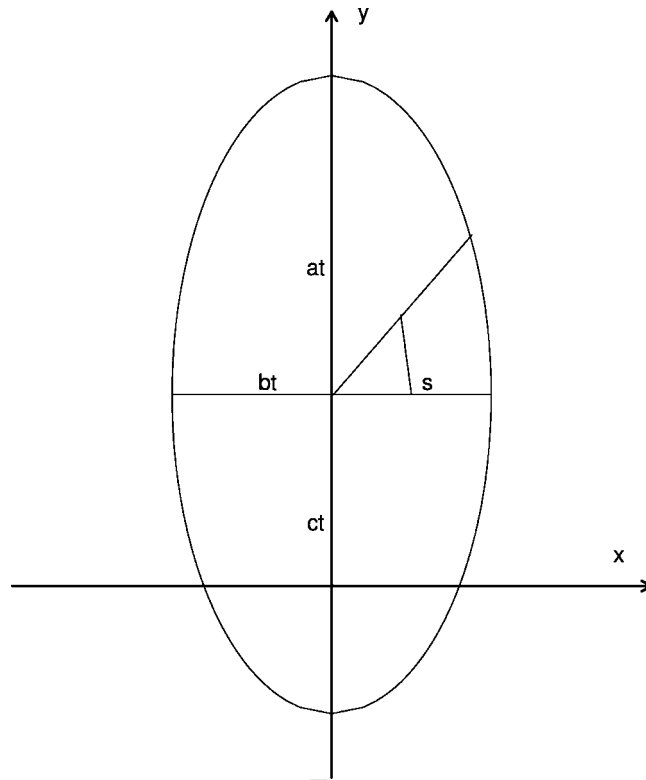


Figure 1. The elliptical shape of fire growth from a point at time  $t$

Under constant conditions for homogeneous fuels, a fire ignited at a point will expand at a constant rate as an ellipse:

$$\begin{aligned}x(s, t) &= bt \cos s \\y(s, t) &= at \sin s + ct\end{aligned}\quad (1)$$

where  $t$  is the time,  $s$  is the counter clockwise angle with respect to the positive  $x$ -axis, the point of ignition is assumed at the origin, and the wind direction is considered to be the positive  $y$ -axis. See Figure 1. The parameters  $a$ ,  $b$  and  $c$  are spatially dependent on  $x$  and  $y$ , and are related to the rates of spread as follows: the forward rate  $v$  is  $a + c$ , the flank rate  $u$  is  $b$  and the back rate  $w$  is  $a - c$ . The rates of spread are obtained from the FBP System.

The coordinates of the fire front at time  $t$  are given by  $(x(s, t), y(s, t))$ , where  $0 \leq s \leq S$ . While the quantity  $s$  defined above is an angle, it will be viewed, from now on, as the arc length parameter, and  $S$  is the length of the entire curve. Let  $\theta$ , a clockwise angle to the  $y$ -axis, represent the wind direction. Then, the ellipse generated by the point  $(x(s, t), y(s, t))$  is at an angle  $\theta$  and defined by Equation (1) where  $t = dt$  and  $a$ ,  $b$  and  $c$  are defined by the fuel, wind and topographical conditions at that point. We take  $dt$  small enough so that  $a$ ,  $b$  and  $c$  remain constant for the time period. Thus, the new fire front at time  $t + dt$  will be the outer envelope of the ellipses generated at each point on the curve at time

$t$ . Having defined the new fire front curve  $(x(s, t + dt), y(s, t + dt))$ ,  $0 \leq s \leq S$ , for finite  $dt$ ; we take the limit as  $dt$  approaches zero to obtain the time derivatives  $x_t(s, t)$  and  $y_t(s, t)$ —Richards' differential spread equations.

### 3. PROMETHEUS: FRONT PROPAGATION APPROXIMATION

While Richards' differential equations are analytically intractable, they can be solved numerically, as in the PROMETHEUS program. As suggested by Richards, Euler's method can be used to solve the pair of ordinary differential equations.

Discretize the curve  $(x(s, t), y(s, t))$  into  $n$  points such that

$$(x_{i,j}, y_{i,j}) = (x(ids, jdt), y(ids, jdt)) \quad (2)$$

where  $ds = 2\pi/n$ , and  $ds$  and  $dt$  are the parameter and time step sizes, respectively, and  $(x_{0,j}, y_{0,j}) = (x_{n,j}, y_{n,j})$ . Using a centered difference in  $s$  and a forward difference in time, we can solve for  $(x_{i,j+1}, y_{i,j+1})$ .

The PROMETHEUS model implements this finite difference solution. First, the initial ignition point is formed as a circle of 32 vertices ordered in a counter clockwise direction. The radius is 1/5th the cell size of the fuel type grid.

We define the following notation:

$\Delta t$  is the duration of the time step applied to a given simulation.  $\Delta t$  is the constant for all time steps.

$\vec{P}_j$  is the vector of points defining the fire front at time iteration  $j$ , equivalently time  $j\Delta t$ .

$P_j^i$  is the  $i$ th point (i.e. the  $i$ th component of  $\vec{P}_j$ ) on the fire perimeter at time iteration  $j$ .

$P_{x_j}^i, P_{y_j}^i, P_{z_j}^i$  are the dimensional components of  $P_j^i$ . Note  $P_{z_j}^i$  is zero in the two-dimensional case for all  $i$  and  $j$ .

$\Delta P_j^i = P_{j+1}^i - P_j^i$  is the change in location of point  $i$  from current time step  $j$  to  $j + 1$ .

$ROS_j^i, FROS_j^i, BROS_j^i, RAZ_j^i$  are the FBP System outputs—ROS (forward rate of spread, formerly  $v$ ), FROS (flank rate of spread, formerly  $u$ ), BROS (back rate of spread, formerly  $w$ ), RAZ (spread direction in azimuth, formerly  $\theta$ ), respectively, for point  $P_j^i$ .

We then find the locations for the  $j + 1$  iteration by solving the following equations:

$$\begin{aligned} \Delta P_{x_j}^i &= \Delta t \frac{b^2 \cos \theta (x_s \sin \theta + y_s \cos \theta) - a^2 \sin \theta (x_s \cos \theta - y_s \sin \theta)}{\sqrt{a^2 (x_s \cos \theta + y_s \sin \theta)^2 + b^2 (x_s \sin \theta + y_s \cos \theta)^2}} + c \Delta t \sin \theta \\ \Delta P_{y_j}^i &= \Delta t \frac{-b^2 \sin \theta (x_s \sin \theta + y_s \cos \theta) - a^2 \cos \theta (x_s \cos \theta - y_s \sin \theta)}{\sqrt{a^2 (x_s \cos \theta + y_s \sin \theta)^2 + b^2 (x_s \sin \theta + y_s \cos \theta)^2}} + c \Delta t \cos \theta \end{aligned} \quad (3)$$

where

$$\begin{aligned} a &= \frac{ROS_j^i + BROS_j^i}{2} \\ b &= FROS_j^i \end{aligned}$$

$$c = \frac{\text{ROS}_j^i - \text{BROS}_j^i}{2}$$

$$\theta = \text{RAZ}_j^i$$

$$2x_s ds = P_{x_j}^{i+1} - P_{x_j}^{i-1}$$

$$2y_s ds = P_{y_j}^{i+1} - P_{y_j}^{i-1} \quad (4)$$

For fixed  $i$  and  $j$ , the forward rate  $\text{ROS}_j^i$  is  $a + c$ , the flank rate  $\text{FROS}_j^i$  is  $b$  and the back rate  $\text{BROS}_j^i$  is  $a - c$ . So, for example, to get  $a$  as above, we take  $(\text{ROS}_j^i + \text{BROS}_j^i)/2 = a$ , and so on.

#### 4. DESCRIPTION OF DATA

The data sets used in this paper are the ROS, FROS, BROS and RAZ values from the Dogrib Fire that threatened Bearberry, Alberta in October 2001. ROS, FROS and BROS are each measured in units of metres/minute; RAZ, the net effective spread direction in azimuth, are measured in degrees, but for consistency in the program used, units are converted to radians. The portion of the terrain considered is  $4950 \text{ m} \times 5800 \text{ m}$ . It is divided into a grid: 232 by 198 grid units, where each grid unit represents 25 square metres. Data values include values that represent non-fuel types such as rivers and lakes, and sloped areas in the terrain.

#### 5. SMOOTHING

We are motivated to smooth the input data for PROMETHEUS in three ways. First, to reduce the measurement error in data: smoothing borrows information from neighbouring observations to reduce noise caused by such errors. While smoothing does introduce some bias, we expect the reduction in variance to more than compensate for this increase. Secondly, to possibly reduce the number of tangles introduced in the solution of the PROMETHEUS equations; smoothing the input data will reduce magnitudes of discontinuities (or derivative discontinuities) which are the likely source of the difficulties encountered by PROMETHEUS. Thirdly, smoothing facilitates a residual-based bootstrap which will introduce stochasticity to the PROMETHEUS model in a natural and theoretically justified manner.

##### 5.1. Our approach

To employ smoothing methods that are readily available and reasonably automatic, we considered `locfit` implemented in R. Among the four candidate variables for smoothing (ROS, FROS, BROS and RAZ), we believe that ROS and RAZ would have the largest effect on the output. This belief is based on some limited simulation runs that were carried out early on in this project. Furthermore, smoothing all input data leads to fire fronts that are sometimes smoother than might be considered realistic. Thus, our attention in this paper is on the effects of smoothing ROS and RAZ.

Upon smoothing these quantities, we use the fitted values (denoted  $\widehat{\text{ROS}}$  and  $\widehat{\text{RAZ}}$ , respectively) as input for the ellipse parameters as given in Equation (4). We then estimate ellipse parameters ( $a$ ,  $c$

and  $\theta$ ) using

$$\begin{aligned}\hat{a} &= \frac{\widehat{\text{ROS}}_j^i + \text{BROS}_j^i}{2} \\ \hat{c} &= \frac{\widehat{\text{ROS}}_j^i - \text{BROS}_j^i}{2} \\ \hat{\theta} &= \widehat{\text{RAZ}}_j^i\end{aligned}\quad (5)$$

To retain the important features of the data, we used the `locfit` function, a non-robust form of local linear regression (see, e.g. Loader, 1999). This procedure relies on a nearest neighbour bandwidth which defines a neighbourhood of the fitting point. This neighbourhood contains the points at which a weighted least squares line is to be estimated. The proportion of points relative to the entire set of points is denoted by the smoothing parameter  $\alpha$ .

Due to autocorrelation in the data, we could not use an automatic smoothing parameter selector. It is well known (e.g. Herrmann *et al.*, 1992) that cross-validation and direct plug-in methods will not work without adjustments that account for the underlying covariance structure. A small smoothing parameter is appropriate for these data since there are regions of rapid change in ROS and RAZ arising from changes in terrain or fueltype. However, taking the smoothing parameter too small leads to lengthy computation times. To meet both standards, our plots of  $\widehat{\text{ROS}}$  are based on a choice of  $\alpha = 0.00025$  which corresponds to a neighbourhood of roughly 10 grid cells, while we used  $\alpha = 0.01$  for  $\widehat{\text{RAZ}}$ . (Other values were studied as well, but we will not report the results here.) See Figures 2 and 3.

We use the log scale to retain consistency of the ROS parameter. Without the log scale, we would introduce an additional bias in the smoothing. Consider, for example a simple case of three rates:  $r_1 = 80$ ,  $r_2 = 40$ ,  $r_3 = 20$ . Notice,  $r_1 = 2r_2$  and  $r_2 = 2r_3$ . If we were to smooth these rates directly, the smoothed values would be  $\hat{r}_1 = \hat{r}_2 = \hat{r}_3 = 140/3 \neq$  true average rate. On the log scale, however, the smoothed rate will be the log of the true average. Also, for fire breaks, the rates of spread are zero.

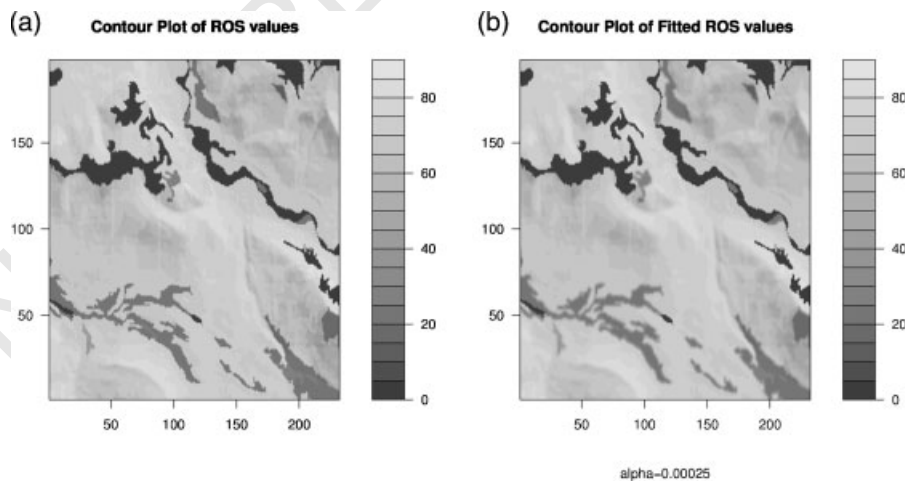


Figure 2. Contour plots for ROS values: (a) shows original ROS values, and (b) shows fitted ROS values when  $\alpha = 0.00025$



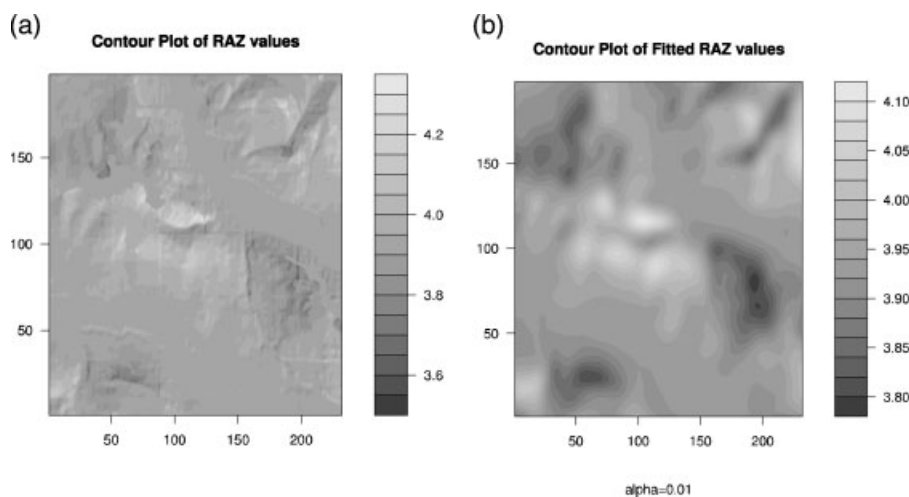


Figure 3. Contour plots for RAZ values: (a) shows original RAZ values, and (b) shows fitted RAZ values when  $\alpha = 0.01$

We delete such observations from the data before applying the smoother. After smoothing, the data are exponentiated, and the fire break observations are appended to the smoothed data set. This approach reduces (but does not entirely eliminate) the tendency for the smoothed values to decrease in approach to such fire breaks. The log scale is not needed for RAZ.

To examine the effects of smoothing these inputs to the PROMETHEUS model, one of the authors designed a PROMETHEUS R version. She followed the algorithm described by Richards in (Richards, 1990), but with some adjustments. In determining which points are *active* or *inactive*, she used the Turning Number Algorithm described by Richards in (Bryce and Richards, 1995), as opposed to the *Scan Line Approach* used in PROMETHEUS. This program will be made available online as an R package.

### 5.2. Does smoothing reduce tangles?

Having determined appropriate alpha values,  $\alpha = 0.002, 0.01, 0.05$ , we tested three cases for smoothing at  $\Delta t = 1, 2, 3$  min. The three cases considered were:

- (1) Smoothing ROS values;
- (2) Smoothing RAZ values;
- (3) Smoothing ROS and RAZ values.

Although the theory states that  $\Delta t$  values should remain small so as to retain consistency in the differential spread equations and reduce tangles, our motivation for large  $\Delta t$  was to show the degree of tangles induced and how smoothing can reduce this even with large  $\Delta t$ . Moreover, we considered the three cases keeping in mind that ROS, the head rate of spread, and RAZ, the net effective wind direction in azimuth, influence the fire front shape the most.

We ran 27 simulations with the combinations produced by the different  $\alpha$ ,  $\Delta t$ , and 3 cases mentioned above. The resulting figures are available on one of the author's websites.



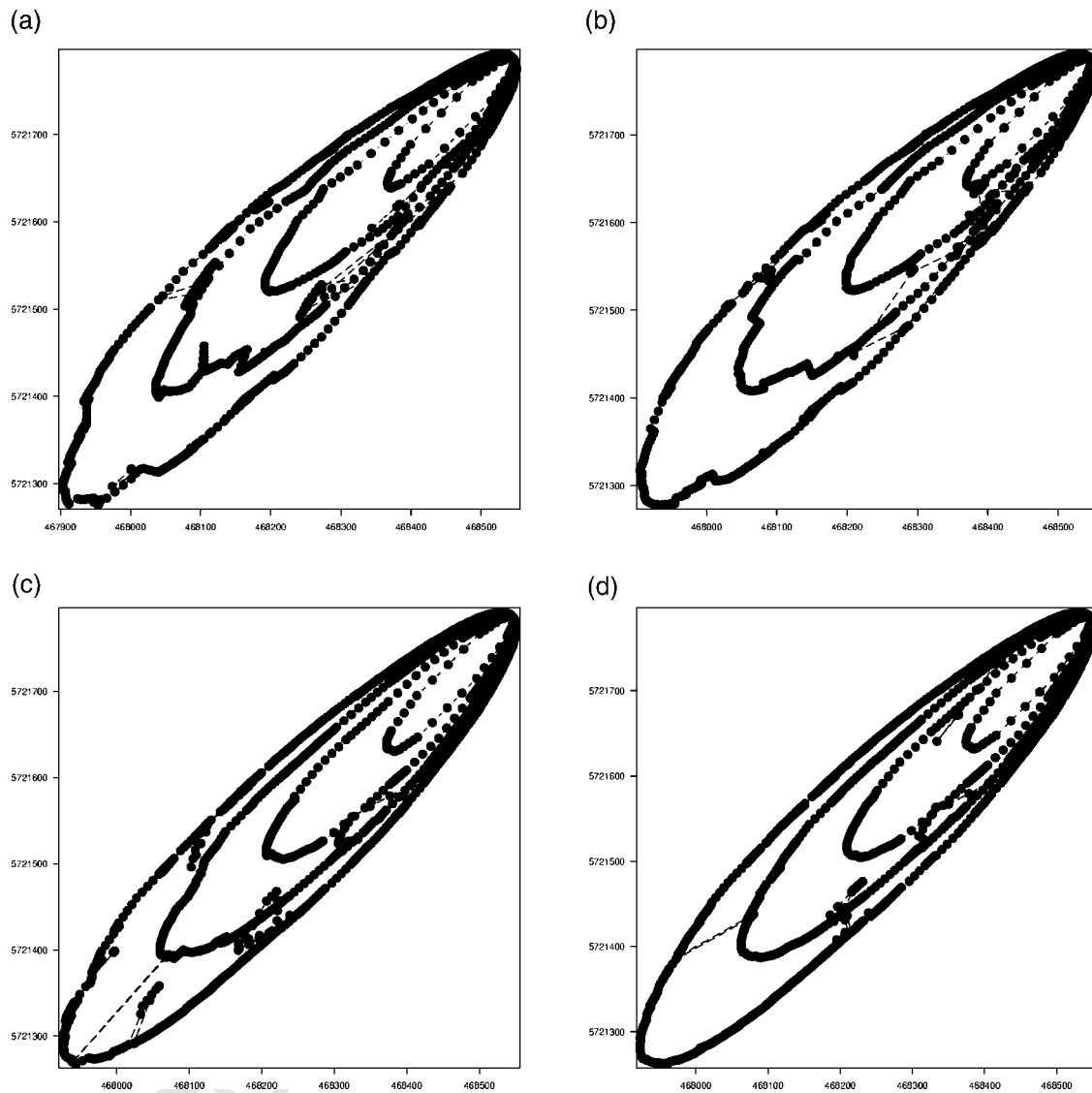


Figure 4. Output for PROMETHEUS R version,  $\Delta t = 3$ ,  $\alpha = 0.01$  (a) non-smoothed data, (b) ROS smoothed only, (c) RAZ smoothed only and (d) ROS and RAZ smoothed

Our results indicate that smoothing the RAZ values often reduces the tangles present, while still maintaining the features of the fire front. However, this is not always the case; occasionally, additional tangles are introduced. See Figure 4.

Smoothing the ROS values also reduces the number of knots induced, often more so than smoothing the RAZ values; compare Figure 4(b) and (c). Smoothing ROS and RAZ together also produces good results; see Figure 4(d). While smoothing ROS and RAZ together does reduce the number of knots, in some instances, the reduction is unrealistic. Notice in Figure 4(d), the fire is nearly a

perfect elliptical shape; this is quite different from the original shape which has a jagged front; see Figure 4(a).

Although not displayed in this paper, with small time steps,  $\Delta t = 1$  and 2 min, the effects of smoothing are not as evident, but are present. The reason for this is that with such small time steps, the likeliness of knots and tangles is small. Due to the few occurrences of tangles, there is only slight room for improvement.

### 5.3. Incorporating stochasticity via the bootstrap

Because the current version of PROMETHEUS is deterministic, we wished to incorporate stochasticity to allow for the eventual computation of probability contours. Our approach is essentially a block bootstrap procedure. Residuals from the smoothing of ROS and RAZ can be resampled and added back to the smoothed surfaces. Because of the autocorrelation in the data, it is inappropriate to use independently, identically distributed resampling of the residuals; resampling blocks of residuals is more appropriate in this setting. The theory for resampling spatial data is not well developed; see Davison and Hinkley (1997) for one account.

*5.3.1. The 2-dimensional block bootstrap.* The idea of the residual block bootstrap that we employ is demonstrated on the RAZ data; a similar treatment applies to ROS, but with some adjustments as described in the next subsection.

The RAZ data are supplied on a grid, so we have measurements  $RAZ_{i,j}$ , for  $i = 1, 2, \dots, m$  and  $j = 1, 2, \dots, n$ . Having smoothed the RAZ data (using the method described earlier or a better alternative), we obtain predicted values at the  $(i, j)$ th grid cell:  $\widehat{RAZ}_{i,j}$ . The  $(i, j)$ th residual is defined as

$$e_{i,j} = RAZ_{i,j} - \widehat{RAZ}_{i,j}$$

Thus, we have an  $m \times n$  grid of residuals. Because of spatial autocorrelation, we resample these residuals using a block approach: the grid is divided into square (or rectangular if preferred) blocks consisting of several grid cells each; each block is replaced by another block (of the same size) randomly selected from the grid of residuals. In algebraic terms, assuming the use of a  $b \times b$  block, we write the  $(i, j)$ th block-resampled residual,  $e_{i,j}^*$  as

$$e_{i,j}^* = e_{i^*+U_{[i/b],[j/b]},j^*+V_{[i/b],[j/b]}}$$

where  $i^* = i(\bmod b)$  and  $j^* = j(\bmod b)$ . The elements of the matrices  $(U_{ij})$  and  $(V_{ij})$ , where  $i = 1, \dots, [m/b]$  and  $j = 1, \dots, [n/b]$ , are independent discrete uniform random variables on  $\{1, 2, \dots, m - b\}$  and  $\{1, 2, \dots, n - b\}$ , respectively. Using these block-randomized residuals, we can add noise back into the smoothed RAZ data:

$$RAZ_{i,j}^* = \widehat{RAZ}_{i,j} + e_{i,j}^*$$

Plugging in these randomized RAZ values (as well as the analogously resampled ROS values) into the equations at (5), we obtain randomized versions of the ellipse parameters  $\hat{a}^*$ ,  $\hat{c}^*$  and  $\hat{\theta}^*$ . Inputting these into the PROMETHEUS model equations at (3) leads to a randomized fire front, possibly quite different from the one based only on the original data.

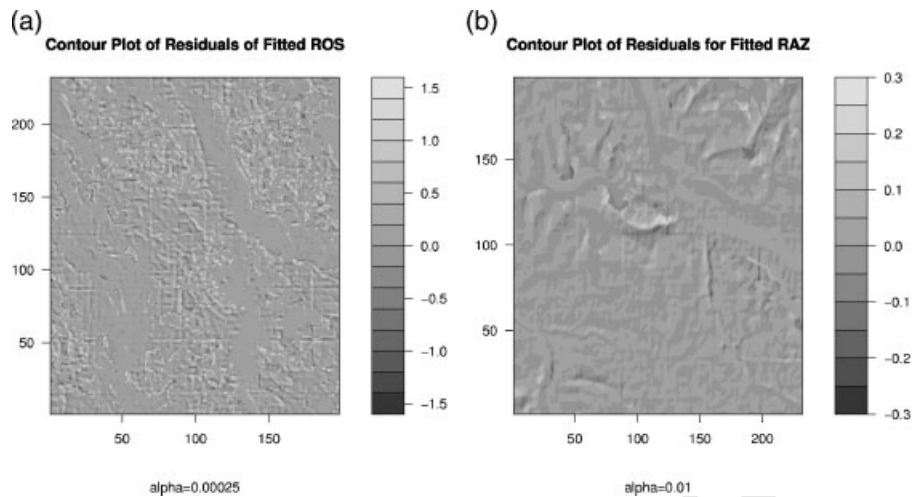


Figure 5. (a) A contour plot of the residuals after fitting ROS using  $\alpha = 0.00025$  in local linear regression; (b) a contour plot of the residuals after fitting RAZ using  $\alpha = 0.01$  in local linear regression

5.3.2. *Handling difficulties with the ROS data.* We found that, especially with respect to ROS, there were some extreme residuals using the smoothing approach described earlier. These extreme residuals could lead to serious distortions and wildly different ellipse parameter values. These residuals are caused by a bimodality in the ROS data: most of the 45 936 observations are in the 60–80 range, but there are several hundred in the 20–30 range as well as several hundred 0's. In order to avoid the distortions caused by this minority of extreme residuals, we set any residual larger than three times the interquartile range to 0. Since these residuals are not caused by noise, but by the lack of fit, our approach seems justified. Moreover, to reduce this lack of fit problem, we considered very small smoothing parameter values for ROS.

A contour plot of the residuals for ROS using  $\alpha = 0.00025$  is displayed in Figure 5(a). Note that with a larger  $\alpha$ , the smoother would have had a great deal of difficulty in capturing the rapid change in the first derivative.

The contour plot of the residuals for RAZ (using  $\alpha = 0.01$ ) is shown in Figure 5(b).

#### 5.4. Results

To introduce randomness to PROMETHEUS as described previously, we considered smoothing at  $\Delta t = 3$  and block sizes = 10, 20 and 40, under the three cases:

- (1) Smoothing ROS values (using  $\alpha = 0.00025$ );
- (2) Smoothing RAZ values (using  $\alpha = 0.01$ );
- (3) Smoothing ROS and RAZ values.

The results for block sizes of 20 and 40 differed slightly from each other; hence Figure 6 only displays results for a block size of 20.

Referring to Figure 6, we observed that, as expected, incorporating randomness in the data values reintroduces knots to the fire front. Observe also that while the fire front shapes were changed due to randomness, the change was not wildly extreme—the basic shape of the original fire front is present. Notice that when both ROS and RAZ are random, the number of knots present is more than when only one is considered random.

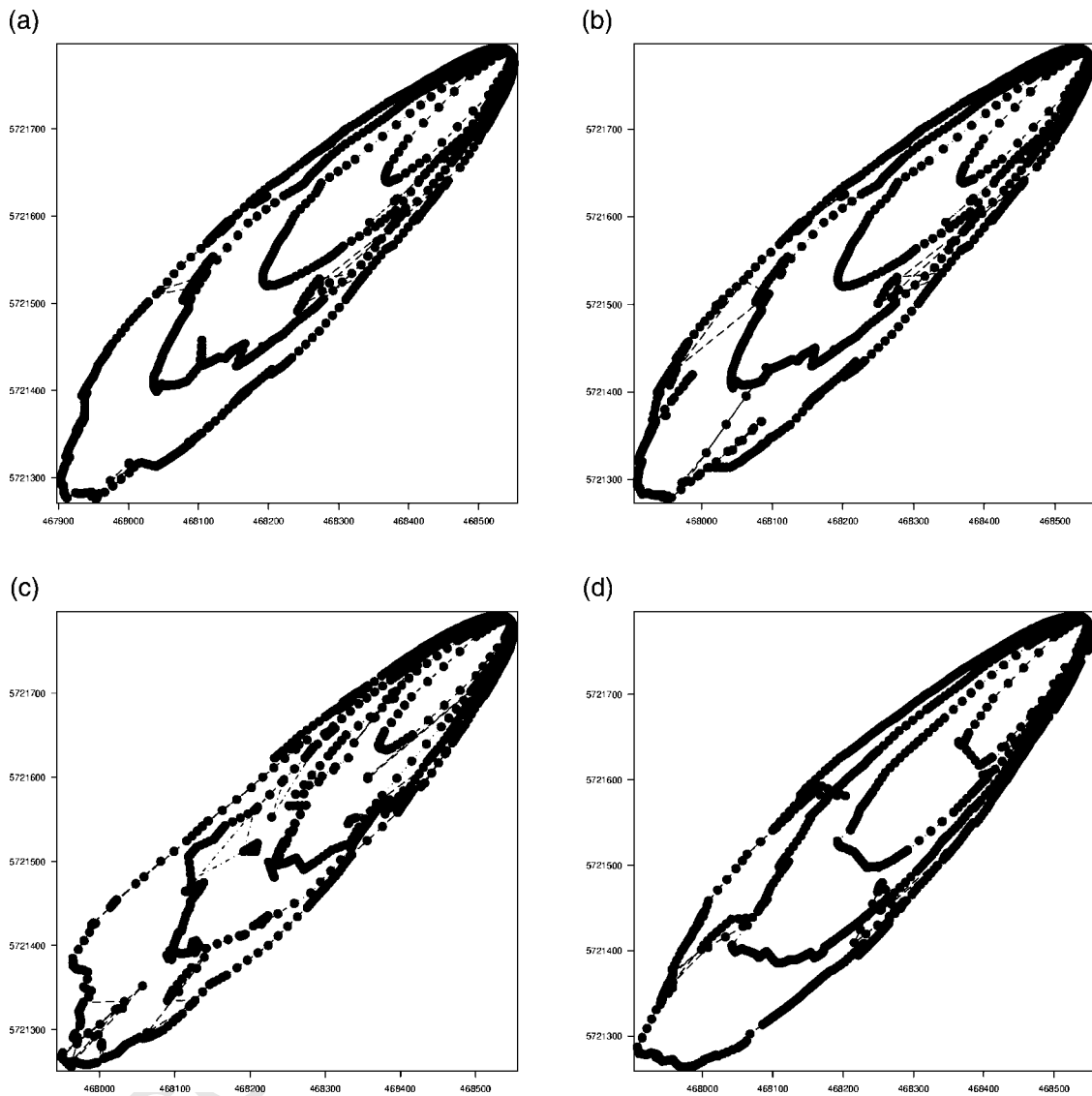


Figure 6. Output for PROMETHEUS R version,  $\Delta t = 3$ , block size = 20 (a) non-random data, (b) random ROS data, (c) RAZ random and (d) ROS and RAZ random

The results here indicate that proceeding in this manner is a good start to introducing stochasticity and should be pursued further.

## 6. CONCLUSIONS

This paper has introduced a variety of issues to be pursued in future research for fire growth simulation. We have constructed a PROMETHEUS R version which can be used for such research.

Our results for smoothing the parameters to reduce knots and tangles is promising and should be pursued. Future work lies in analyzing the smoothing using goodness of fit tests and with other sets of input data. We have presented a fairly naive approach to the two-dimensional smoothing problem; further work is required to properly handle the sharp ridges and valleys in the data. Spatial autocorrelation will also require attention in a more careful implementation. The RAZ data are actually angular data, so this will require a different implementation as well. Our goal has been to demonstrate the main effects of smoothing on the evolution of the fire front; better smoothing methods will be required when this is actually implemented in practice.

Although smoothing has reduced the tangles, we ultimately would like a way to identify the tangles and remove them. A promising new algorithm is currently being tested; it will be described in a forthcoming report from the Pacific Institute for the Mathematical Sciences (PIMS). Ultimately, the combination of using smoothing to reduce tangles and then the algorithm to remove them altogether would assist greatly in the accuracy of a fire growth model.

Our introduction of stochasticity to the model should also be pursued further. We have shown in this paper that it is possible to add randomness to the deterministic PROMETHEUS algorithm in a natural and reasonable way. We have achieved this without changing the inherent properties of the model, unlike all other attempts that have been made at producing stochastic fire growth models. The residual resampling approach taken here is a form of block bootstrap which rests on some theory; this is a sound method for dealing with the autocorrelation which underlies the data. Further work is required to verify that this application of the block bootstrap is completely justified and to fine-tune the implementation.

We have not presented probability contours for the possible spread of the fire in this paper for the reason that we believe this to be premature. In the absence of proper model assessment with real fire perimeters, actual numerical probability values will be possibly misleading. What we have shown is how adding stochasticity can alter the shape of the fire front.

While the PROMETHEUS model is an excellent tool for fire management, it offers numerous avenues for further exploration; we hope that the preliminary results of this paper encourage others to join in this adventure.

#### ACKNOWLEDGEMENTS

WJB acknowledges the support of the Natural Sciences and Engineering Research Council of Canada through NSERC Discovery Grant 138127-2004. This work was also supported in part by GEOIDE, a network centre of excellence in Sustainable Forest Management as well as by the PROMETHEUS project, which is run by the Government of Alberta. This work was an outgrowth of a PIMS industrial problem-solving workshop held at Simon Fraser University in June 2006, in which a team of researchers studied aspects of the PROMETHEUS algorithm. The authors of the present paper acknowledge helpful conversations with the members of this team: Jared Barber, Chris Bose, Anne Bourlioux, Eric Brunelle, Thomas Hillen, Clement Lam, Ben Ong, Christiane Poeschl and Lutong Zhou.

#### REFERENCES

- Alexander ME. 1985. Estimating the length-to-breadth ratio of elliptical forest fire patterns, *Eighth Conference on Fire and Forest Meteorology*, Society of American Foresters.
- Bryce R, Richards G. 1995. A computer algorithm for simulating spread of wildland fire perimeters for heterogeneous fuel and meteorological conditions. *International Journal of Wildland Fire* 5: 73–79.
- Davison A, Hinkley D. 1997. *Bootstrap Methods and Their Application*. Cambridge University Press: Cambridge.
- Fons W. 1946. Analysis of fire spread in light forest fuels. *Journal of Agricultural Research* 72: 93–121.

- 1  
2  
3  
4 Forestry Canada Fire Danger Group. 1992. Development and structure of the Canadian Forest Fire behaviour Prediction System. Forestry Canada, Ottawa, Ontario. *Information Report ST-X-3*.
- 5 Gillett NP, Weaver AJ, Zwiens FW, Flannigan MD. 2004. Detecting the effect of climate change on Canadian forest fires. *Geophysical Research Letters* **31**: L18211, doi:10.1029/2004GL020876.
- 6 Herrmann E, Gasser T, Kneip A. 1992. Choice of bandwidth for kernel regression when residuals are correlated. *Biometrika* **79**:  
7 783–796.
- 8 Loader C. 1999. *Local Regression and Likelihood*. Springer: New York.
- 9 Podur J, Martell DL, Knight K. 2002. Statistical quality control analysis of forest fire activity in Canada. *Canadian Journal of  
10 Forest Research* **32**: 195–205.
- 11 Richards G. 1995. A general mathematical framework for modelling two-dimensional wildland fire spread. *International Journal  
12 of Wildland Fire* **5**: 63–72.
- 13 Richards G. 1990. An elliptical growth model of forest fire fronts and its numerical solution. *International Journal for Numerical  
14 Methods in Engineering* **30**: 1163–1179.
- 15 Richards G. 1988. Numerical simulation of forest fires. *International Journal for Numerical Methods in Engineering* **25**: 625–634.
- 16  
17  
18  
19  
20  
21  
22  
23  
24  
25  
26  
27  
28  
29  
30  
31  
32  
33  
34  
35  
36  
37  
38  
39  
40  
41  
42  
43  
44  
45  
46  
47  
48  
49  
50  
51  
52  
53  
54  
55  
56

1  
2  
3  
4  
5  
6  
7  
8  
9  
10  
11  
12  
13  
14  
15  
16  
17  
18  
19  
20  
21  
22  
23  
24  
25  
26  
27  
28  
29  
30  
31  
32  
33  
34  
35  
36  
37  
38  
39  
40  
41  
42  
43  
44  
45  
46  
47  
48  
49  
50  
51  
52  
53  
54  
55  
56

## Author Query Form (ENV/907)

**Special Instruction: Author please include responses to queries with your other corrections and return by e-mail.**

Q1: Author: Please check the suitability of suggested short title.

UNCORRECTED PROOFS